A Model Study of the Role of Convection in Westerly Wind Burst Dynamics

MINMIN FU[a] AND ELI TZIPERMAN[b]

[a] *Department of Earth and Planetary Sciences, Harvard University, Cambridge, Massachusetts*
[b] *Department of Earth and Planetary Sciences, School of Engineering and Applied Sciences, Harvard University, Cambridge, Massachusetts*

(Manuscript received 11 September 2020, in final form 24 April 2021)

ABSTRACT: Westerly wind bursts (WWBs) are anomalous surface wind gusts that play an important role in ENSO dynamics. Previous studies have identified several mechanisms that may be involved in the dynamics of WWBs. In particular, many have examined the importance of atmospheric deep convection to WWBs, including convection due to tropical cyclones, equatorial waves, and the Madden–Julian oscillation. Still, the WWB mechanism is not yet fully understood. In this study, we investigate the location of atmospheric convection which leads to WWBs and the role of positive feedbacks involving surface evaporation. We find that disabling surface flux feedbacks a few days before a WWB peaks does not weaken the event, arguing against local surface flux feedbacks serving as a WWB growth mechanism on individual events. On the other hand, directly suppressing convection by inhibiting latent heat release or eliminating surface evaporation rapidly weakens a WWB. By selectively suppressing convection near or farther away from the equator, we find that convection related to off-equatorial cyclonic vortices is most important to equatorial WWB winds, while on-equator convection is unimportant. Despite the strong resemblance of WWB wind patterns to the Gill response to equatorial heating, our findings indicate that equatorial convection is not necessary for WWBs to develop. Our conclusions are consistent with the idea that tropical cyclones, generally occurring more than 5° away from the equator, may be responsible for the majority of WWBs.

KEYWORDS: Deep convection; Tropical cyclones; Wind bursts; Intraseasonal variability

1. Introduction

Westerly wind bursts (WWBs) are episodic, anomalous equatorial westerly wind anomalies, which can result in local reversals of the trade winds. Previous studies have defined them as events with an anomalous wind strength exceeding 5–7 m s^{-1} over a zonal extent of at least 10°, and meeting the above criteria for at least 2–5 days. Following the definitions above, they occur about 5–15 times per year (Hartten 1996; Harrison and Vecchi 1997; Yu et al. 2003; Seiki and Takayabu 2007). The identified events, however, are generally characterized by a larger zonal extent of 30°–40° longitude, and can persist for as long as 2 weeks (Harrison and Vecchi 1997; Vecchi and Harrison 2000). WWBs occur mostly in the western-central tropical Pacific, and only rarely in the eastern tropical Pacific. They are also known to occur much more frequently during El Niño events compared to La Niña events.

WWBs occurring along the equator are an important component of high-frequency atmospheric wind variability in the tropics, and critically participate in ENSO dynamics by exciting eastward propagating downwelling Kelvin waves that influence developing El Niño events (McPhaden et al. 1992; Kessler et al. 1995). Initially, WWBs were believed to be stochastic events that trigger El Niño events, possibly via nonnormal amplification (Penland and Sardeshmukh 1995; Kleeman and Moore 1997; Moore and Kleeman 1997a,b, 1999, 2001). However, careful analysis shows that these events are correlated with the SST and appear to develop in response to the beginning of a warming event (Yu et al. 2003; Tziperman and Yu 2007). Thus, the Kelvin waves excited by WWBs, which have been shown to cause warming in the eastern Pacific (Giese and Harrison 1991) and have been associated with the onset and amplification of El Niño events (Luther et al. 1983; Latif et al. 1988; Perigaud and Cassou 2000; Lengaigne et al. 2004), are most likely amplifying warm events that are already developing (Eisenman et al. 2005), and this understanding makes it possible to develop WWB parameterizations for ENSO models (Gebbie et al. 2007; Gebbie and Tziperman 2009a,b). WWBs are therefore perhaps best described as state-dependent, or multiplicative, stochastic events (Jin et al. 2007; Perez et al. 2005; Sura and Sardeshmukh 2008).

WWBs have been proposed to be caused by cold surges from midlatitudes (Chu 1988), single and paired tropical cyclones (Keen 1982; Nitta 1989; Lian et al. 2018a), and convectively coupled Rossby waves (Kiladis and Wheeler 1995; Puy et al. 2016) and seem to be modulated by the Madden–Julian oscillation (MJO; Chen et al. 1996; Zhang 1996; Seiki and Takayabu 2007; Chiodi et al. 2014; Feng and Lian 2018). A common feature of all the above WWB theories is the importance of atmospheric deep convection (e.g., Meehl et al. 1996; Hartten 1996; Fasullo and Webster 2000). For instance, Hartten (1996) found that deep convection is present within 10°–15° longitude and latitude of most WWBs. In terms of the spatial location of the related convection, some work has focused on near-equator convection, generally within ±5° latitude of the equator (e.g., Kiladis et al. 1994; Fasullo and Webster 2000). This body of literature has often studied WWBs in relation to equatorially trapped disturbances such as the MJO and convectively coupled equatorial waves (CCEWs). A recent study found that the convective phase of the MJO nearly doubles the

Corresponding author: Minmin Fu, mjfu@g.harvard.edu

DOI: 10.1175/JCLI-D-20-0723.1

probability of a WWB occurring (Feng and Lian 2018). Another subset of the literature instead focuses on the importance of tropical cyclones (TCs; Keen 1982; Lian et al. 2018a), whose centers are usually located further than 5° latitude from the equator. It has been found that approximately 70% of WWBs in the western tropical Pacific can be associated with individual or paired tropical cyclones (Lian et al. 2018a). Finally, the double-cyclone structure associated with strong WWBs has frequently been compared (and contrasted) to the stationary Rossby wave pattern of the Gill response to an equatorial heat source (Gill 1980; Fu and Tziperman 2019; Hartten 1996; Seiki and Takayabu 2007; Harrison and Giese 1991; Levine et al. 2017; Kubota et al. 2006; Lander 1990). However, there remains ambiguity to the precise nature of the convection which generates WWBs. Is it the on-equator convection (e.g., Gill response to a convective outburst) or off-equator convection (e.g., tropical cyclogenesis) that is most vital to WWB development?

The objective of this paper is to investigate the importance of surface evaporation and deep convection to the dynamics of equatorial WWBs, in particular the role of positive feedbacks and the spatial position of the convection responsible for the WWBs. In a previous paper (Fu and Tziperman 2019), it was found that when the wind-induced surface heat exchange (WISHE) mechanism was turned off in an aquaplanet simulation, the number of WWBs went down significantly. In addition, latent heat fluxes were found to be very strong 1–2 days before and after the peak of the event. That suggested that WISHE may serve as a growth mechanism for individual WWBs, whereby westerly anomalies could increase surface wind speeds, enhancing evaporation and convection, hence further strengthening the anomalous surface westerlies. In this paper, we further examine the importance of convective heating and surface fluxes to the development of individual events through a series of initial value experiments. We find that while WISHE seems to be enhancing the overall occurrence of WWBs in some model configurations, it does not play a direct role in the growth mechanism of individual events, at least during the 2–4 days prior to the peak of the event. Furthermore, our experiments provide additional insight into the role that convection plays in WWB dynamics. We design a series of GCM experiments where we selectively suppress convection near and away from the equator, around developing WWBs and find that convection close to the equator is unimportant for explaining the WWB growth. Our results indicate that double cyclones associated with WWBs should not simply be considered as a Gill response to on-equator heating, since suppressing convection on the equator starting a few days prior to the event, either through disabling evaporation or convective heating, fails to disable a developing event. Suppressing tropical convection away from the equator, on the other hand, at around ±(3°–13°) latitude, is found to considerably weaken WWB winds. This supports the idea that cyclonic vortices associated with deep convection off the equator may be the main process driving WWBs, in agreement with Lian et al. (2018a).

Section 2 introduces the methodology, including datasets, model configuration, and WWB detection criteria. Section 3 describes the results of our experiments where we selectively modify surface fluxes and moist diabatic heating a few days before individual WWBs. Here we present evidence against a local WISHE feedback, and discuss the importance of off-equator convection. We conclude in section 4.

2. Methods

We use model output and reanalysis to study WWBs under realistic conditions. For initial diagnostics of model WWBs, we use the Community Earth System Model Large Ensemble Project (CESM-LE), which consists of a 40-member ensemble of fully coupled GCM simulations (Kay et al. 2015). Simulations are run at a 1° longitude/latitude grid with the Community Atmosphere Model (CAM) version 5.2 as the atmospheric component, and are subject to historical radiative forcing during the period of 1920–2005, the 85-yr period that is used in this paper. The large number of ensemble members allows many events to be identified and composited.

Separate from the CESM-LE dataset, we also utilize a 60-yr run of CESM 1.2.2.1 with CAM4 as its atmospheric component. The finite-volume core is used, with a resolution of 1.25° in longitude and 0.9° in latitude. Versions of CAM later than CAM3 use improved convection schemes that are expected to simulate WWBs reasonably well (Lian et al. 2018b). Deep convection in CAM4 utilizes the parameterization scheme of Zhang and McFarlane (1995), based on a plume ensemble approach. When the atmosphere is conditionally unstable, updrafts exponentially eliminate the instability over a specified time scale. For reanalysis, we use ERA-Interim (ERA-I), a global atmospheric reanalysis, from 1979 to 2019 (Dee et al. 2011).

In this paper, westerly wind bursts are defined as episodes of anomaly zonal wind averaged between ±5° latitude, exceeding 5 m s^{-1} over a longitude spanning more than 10° longitude, and meeting the above criteria for at least two consecutive days. All anomaly fields refer to differences relative to the seasonal climatology and are computed by subtracting the daily-averaged seasonality. Although other studies have discussed the effect of filtering winds (e.g., Puy et al. 2016; Feng and Lian 2018), in this study, no filtering in space or time is applied to the data, as our simulation does not use a dynamical ocean and is not expected to generate strong interannual variability. The central longitude and date are defined as the day and longitude of the maximum WWB zonal wind anomaly within an individual event. In our 60-yr control run of CESM, 4.1 WWBs per year are identified on average in the Pacific basin. Out of these, 25 individual events are identified between the longitudes of 160° and 170°E over the course of this 60-yr simulation. The longitude band is narrower than those used by Harrison and Vecchi (1997), to avoid zonal smearing of the composited events. We focus on these longitudes because WWBs most frequently happen in this region of the western-central equatorial Pacific.

3. Results

We first show initial analyses that suggest that WISHE might be an amplifying mechanism for WWBs happening in the

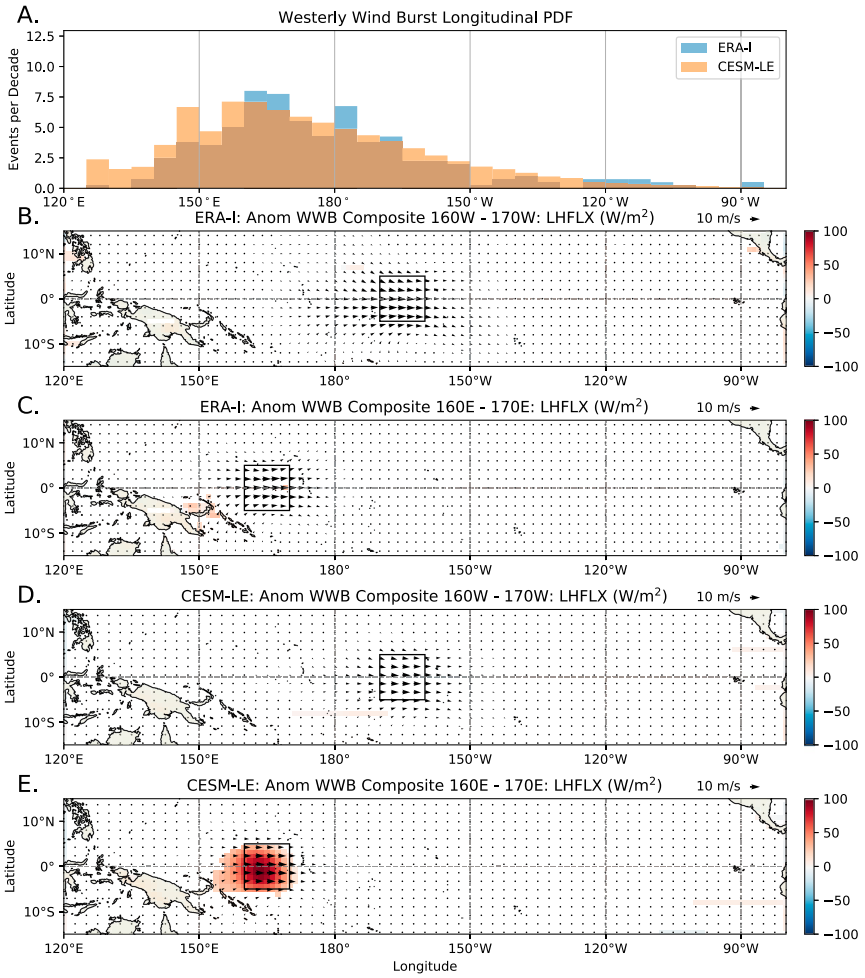

FIG. 1. (a) Longitudinal WWB frequency distribution, and composites of WWBs between (b),(d) 160° and 170°W and between (c),(e) 160° and 170°E showing their anomaly surface wind field and latent heat fluxes. Shown in (a) are histograms of the longitudinal distribution of WWBs in units of WWBs per decade for two datasets with a bin width of 5° longitude. Histograms are constructed for ERA-I reanalysis (blue) and the CESM large ensemble (orange). WWB composites in (b) and (c) are constructed from ERA-I reanalysis from 1979 to 2019, while composites in (d) and (e) are constructed from the CESM Large Ensemble. Black boxes in (b)–(e) show regions where WWBs are composited.

western-central tropical Pacific, and a damping for those happening farther east, seemingly consistent with Fu and Tziperman (2019). Later, though, we show that individual events are not, in fact, amplified by WISHE. To investigate the role of WISHE, we first utilize CESM-LE. To verify that CESM accurately simulates WWB statistics (e.g., Lian et al. 2018b), we plot in Fig. 1a the longitudinal probability density function (PDF) of WWB frequency in both CESM-LE and ERA-I. In both reanalysis and CESM-LE, WWBs are most likely to occur in the western-central tropical Pacific between 150°E and 180°, and their probability of occurring decreases strongly toward the eastern tropical Pacific.

To investigate the difference between those WWBs occurring in the west versus central Pacific, we composite WWBs occurring at two different longitude intervals in Figs. 1b–e. Because of the importance of surface evaporation flux to the overall statistics of WWBs (Fu and Tziperman 2019), we focus on the surface latent heat flux here. Figures 1b–e show that, in both CESM-LE and reanalysis, events occurring west of around 180° are on average characterized by strong positive latent heat flux anomalies, while those occurring to the east are not. For instance, Figs. 1c and 1e show composites of WWBs between 160° and 170°E, which are associated with strong anomalous latent heat fluxes. This is because strong westerly anomalies superimposed on the weak easterly trade winds in this region lead to large absolute westerlies, which enhance surface wind speeds and surface fluxes. On the other hand, those events occurring between 160° and 170°W (Figs. 1b,d) are not associated with surface evaporation anomalies because the easterly trade winds are much stronger in this region. Westerly

anomalies superimposed on strong trade winds, on the other hand, tend to merely weaken the strong trades and are unlikely to increase the absolute surface wind speed. The anomaly latent heat flux fields are qualitatively similar between CESM-LE and ERA-I reanalysis. If individual WWBs were to be amplified by a WISHE mechanism, this could potentially explain the stronger and more frequent WWBs in the western-central tropical Pacific, although we now show WISHE turns out not to be an amplifying mechanism of individual WWBs.

Next, to examine if individual WWBs are, in fact, amplified by WISHE, we perform a series of experiments to probe the importance of evaporation and convection, on and off the equator, to the development of WWBs. For this purpose, we selectively modify evaporation and latent heat release in specific regions. The model surface fluxes and convective heating are set to climatology in these regions n days before the peak of an individual WWB occurs, and the effects on the subsequent evolution of the WWB are examined. This overwrites the model-computed values with climatology values independent of time. To do this systematically, we define a set of three 30°-longitude-wide boxes (shown in Fig. 3, top row, center and right columns) surrounding the central longitude of 165°E, one on the equator (3°S–3°N) and two off the equator (3°–13°N, 3°–13°S).

First, to examine the importance of surface flux feedbacks to WWB dynamics, we set the latent heat fluxes to the annual mean climatology within the entire area covered by the three boxes at either 2 or 4 days before day 0 (the day of maximum westerly wind anomaly) for the 25 WWBs located between 160° and 170°E (defined in section 2). Then, the zonal wind anomalies are averaged between ±5° latitude and the maximum anomaly between 155° and 175°E is plotted as a function of time relative to the day of peak WWB wind strength (Fig. 2a). We find that the WWB development and growth are not halted, and the event reaches its peak amplitude, regardless of whether the interactive latent heat fluxes are disabled 2 or 4 days before the peak. The results of the experiment done here show that WISHE is not needed for sustaining and amplifying individual WWB events once they have begun.

However, when latent heat fluxes are set to zero, rather than to climatology, in the domain covered by the boxes, the WWB is considerably weakened (Fig. 2b). This can be explained by the expected weakening of convection caused by the absence of surface evaporation. The event is further suppressed when the fluxes are removed 4 days rather than 2 days before the event peak. This suggests that there is a delay between evaporation of moisture and its condensation/latent heat release, which strengthens the event, as is further tested next. We conclude that interactive latent heat fluxes (i.e., WISHE) do not appear to act as a local feedback or growth mechanism for these individual events once they have started, although the climatological evaporation must be present to sustain the convection necessary for WWBs.

Next, we perform the related experiment of directly setting the convective heating from the CESM deep convection scheme (output variable ZMDT) to climatology (Fig. 2c) or to zero (Fig. 2d), by overwriting the model values throughout the entire region covered by the three boxes, at all vertical levels, either 2 or 4 days before day 0. This replaces the heating tendency in the region with a fixed vertical profile that is independent of time. As a result, the positive feedback leading to atmospheric convection is eliminated, and no convection is expected in this region (Fig. 3). This experiment achieves a similar result; in both cases (2 or 4 days) the equatorial westerly anomalies weaken drastically and immediately, and cause the event to no longer meet the WWB threshold. This experiment confirms that deep convection plays a crucial role in the development of a WWB. These results are in agreement with the fact that convection is known to occur in association with WWBs, in both observations (Hartten 1996; Fasullo and Webster 2000) and numerical simulations (Fu and Tziperman 2019; Lian et al. 2018b).

We have now found that interactive surface fluxes are unimportant to the development of an individual WWB, but that directly suppressing convection, by either eliminating moist convective heating or surface evaporation, dramatically weakens the event. We can now direct our attention to the spatial position of the surface latent heat fluxes and convection, which lead to the WWB development. We perform the experiments of setting latent heat flux to zero in the on-equator boxes and in the off-equator boxes separately to better understand the spatial location of the convection that is necessary for causing the WWBs. In Figs. 2e and 2f, we again plot the maximum zonal wind anomaly between 155° and 175°E at various days before and after the peak of the individual events and demonstrate that only suppressing evaporation *off* the equator weakens the WWB. When convection is suppressed on the equator, the events are slightly weakened (Figs. 2e,g), but much less than for the off-equator experiments (Figs. 2f,h). The same result—that only suppressing the convection away from the equator strongly weakens the event—is found for setting the convective heating or surface evaporation to zero (Figs. 2e–h).

To investigate the changes that cause the WWBs to weaken, we plot the changes to the wind fields and convective precipitation caused by the experiments of disabling convective heating (described above). The effect of disabling deep convection on or off of the equator for individual events is shown in Fig. 3. First, the convective precipitation and surface wind fields for a composite and five individual events, at day 0, are shown on the left column for reference. Next, the surface wind changes and full precipitation fields that result from convective heating being disabled on-equator (center column) or off-equator (right column) two days prior to the peak of the events are plotted. From the composites (first row), we observe that consistent with our expectations, convective precipitation is decreased in the region where convective heating has been disabled. Virtually no precipitation occurs in the regions where convective heating has been set to zero, consistent with the fact that such a procedure effectively eliminates convective instability. Furthermore, we observe that the westerly anomalies are greatly weakened when convection is suppressed off-equator (right column) but not on-equator (center column). From individual events in the following rows, we show that WWBs are associated with a variety of different convection patterns both on and off the equator. For some of the events,

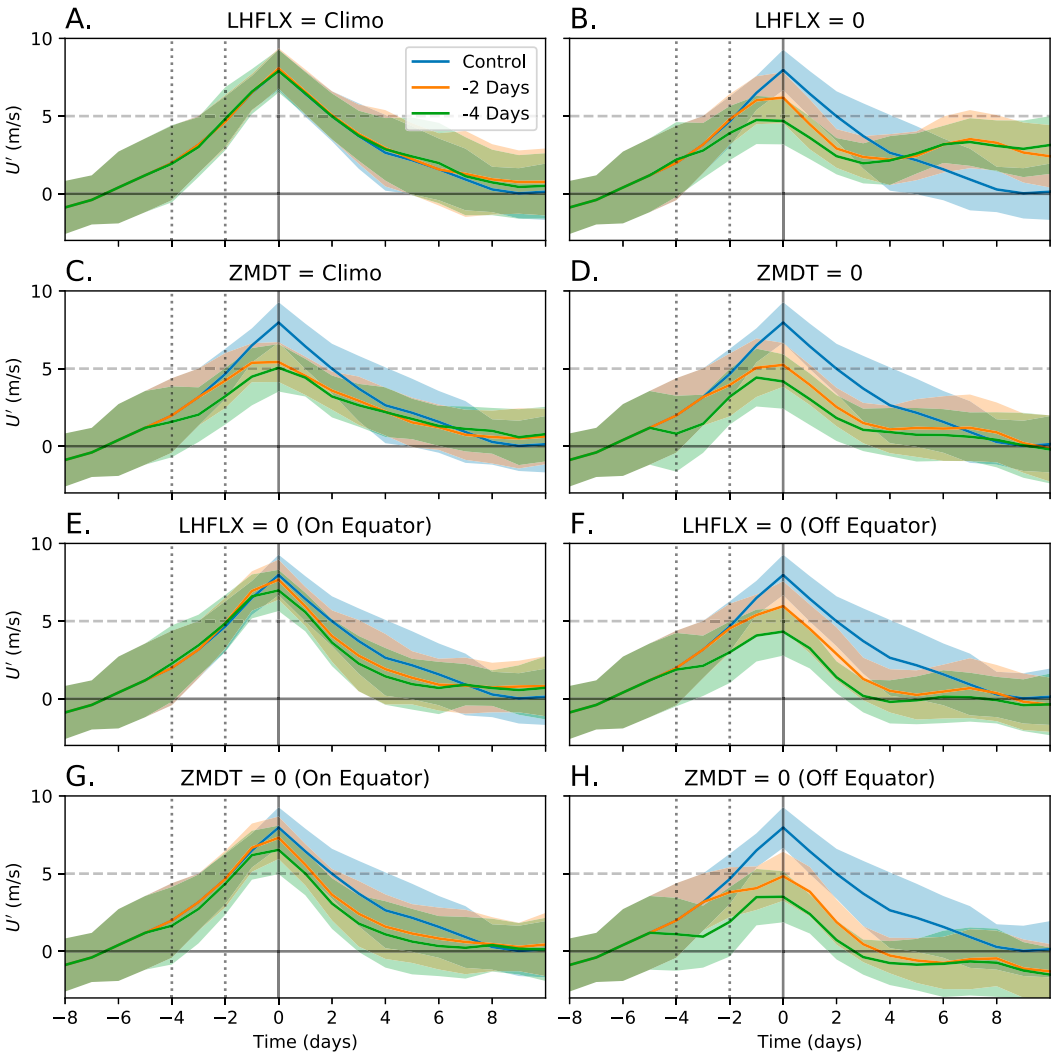

FIG. 2. Composited maximum WWB zonal wind anomalies between 155° and 175°E as a function of time for the control simulation (blue), and for experiments where surface fluxes or convective heating are modified starting at day −2 (orange) or day −4 (green). The plotted curve indicates the mean, and the shaded region corresponds to ±1 standard deviation of the 25 ensemble members. (a),(b) Experiments where surface latent heat fluxes in the three-box domain (see section 2) are set to climatology or to zero, respectively. (c),(d) Experiments where the heating from the deep convection scheme is set to climatology or to zero, respectively. Also shown are results when (e),(f) latent heat fluxes are set to zero near the equator and off the equator, respectively, and (g),(h) the convective heating rather than latent heat fluxes is set to zero.

the convection is concentrated in a patch and results in a clear cyclone (e.g., Fig. 3, rows 2 and 5, left column). In other events, the convection is more spread out and the presence of a cyclone is more ambiguous (e.g., Fig. 3, rows 3 and 6, left column). We find that eliminating surface evaporation leads to qualitatively similar results (not shown).

Next, we evaluate the role of convection and cyclones by plotting the anomalous surface winds and surface vorticity of WWBs in Fig. 4. By comparing individual events (cf. left columns in Figs. 3 and 4), we observe that convective precipitation is correlated with cyclonic surface vorticity. In all five individual events in the control simulation, relatively strong cyclonic surface vorticity is observed both north and south of the equator, at around 5°N and 5°S. When convection is disabled on the equator, the few events involving cyclones very close to the equator are impacted (e.g., row 6). However, the majority of events involve cyclones located farther than 5° from the equator (e.g., rows 2, 3, and 5), and disabling convection *near the equator* (within ±3° latitude) has little effect on these events, as the *off-equator* vorticity associated with these events does not change. This is consistent with the fact that vorticity is small near the equator due to the weak Coriolis force. On the other hand, disabling the convection off-equator virtually eliminates vorticity in the specified boxes, drastically

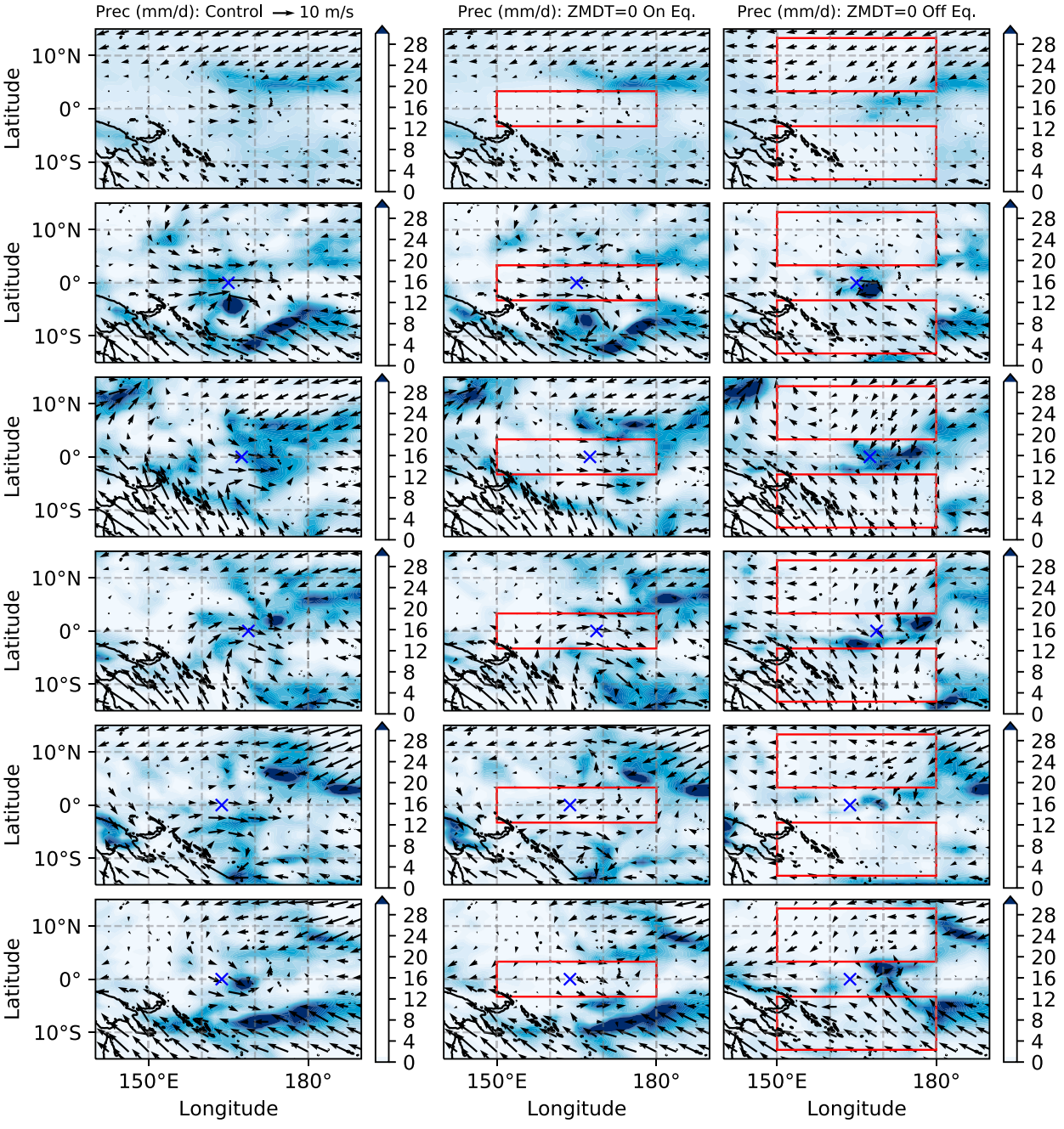

FIG. 3. Surface wind field (arrows) and convective precipitation (shading) for WWBs between 160° and 170°E at day 0. (left) The control experiment. Two days before day 0, convective heating is disabled (center) near the equator or (right) off the equator. Difference in surface winds from control is shown in the center and right columns; full convective precipitation rate is shown in all panels. The first row shows a composite, and rows 2–6 show the five strongest individual events. The longitudinal position of the WWB center in the control simulation is marked by a blue cross. In the center and right columns of row 1, arrows are shown where either zonal or meridional wind differences are statistically significant to a 95% confidence level by Student's *t* test.

weakening the WWB. We note that sometimes the cyclones that were originally within the off-equator boxes re-emerge closer to the equator, leading to a strongly weakened, albeit not totally eliminated westerly anomaly (e.g., rows 4 and 6). Since WWB are defined near the equator, and their wind anomalies do not extend beyond 10° latitude, the fact that the climatological southeasterly (northeasterly) winds from the south (north) of equator must turn to become westerlies near the equator during a WWB is consistent with the vortices we observe at around 5°N and 5°S.

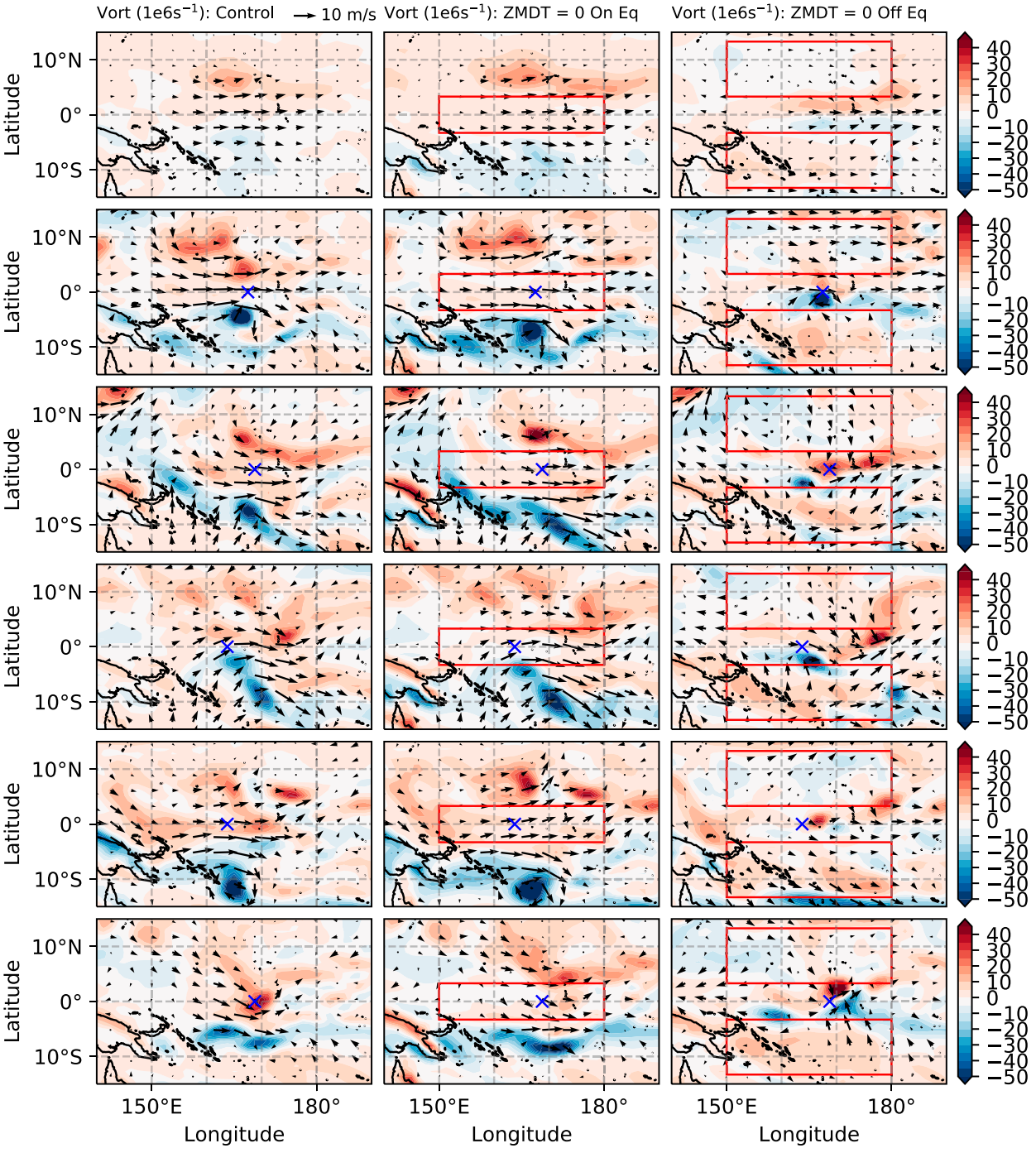

FIG. 4. Anomaly surface wind field (from climatology; arrows) and anomaly surface wind vorticity (from climatology; shading) for WWBs occurring between 160° and 170°E at day 0. (left) The control experiment. Two days before day 0, convective heating is turned off (center) near the equator or (right) off the equator. The region in which convection is suppressed is indicated by the red boxes. The longitudinal position of the WWB center in the control simulation is marked by a blue cross. The first row is a composite of the 25 events, and rows 2–6 show the five strongest individual events.

We note there is uncertainty regarding the relevance of our results to observed WWBs. To look into this, we plotted the anomalous convective precipitation and surface winds for composites and five strongest events in both CESM and reanalysis. The results can be compared in Fig. 5, suggesting that the off-equator variability is a signature of both model and observed WWBs. It is, however, difficult to tell based on that alone that convection off the equator is the key WWB

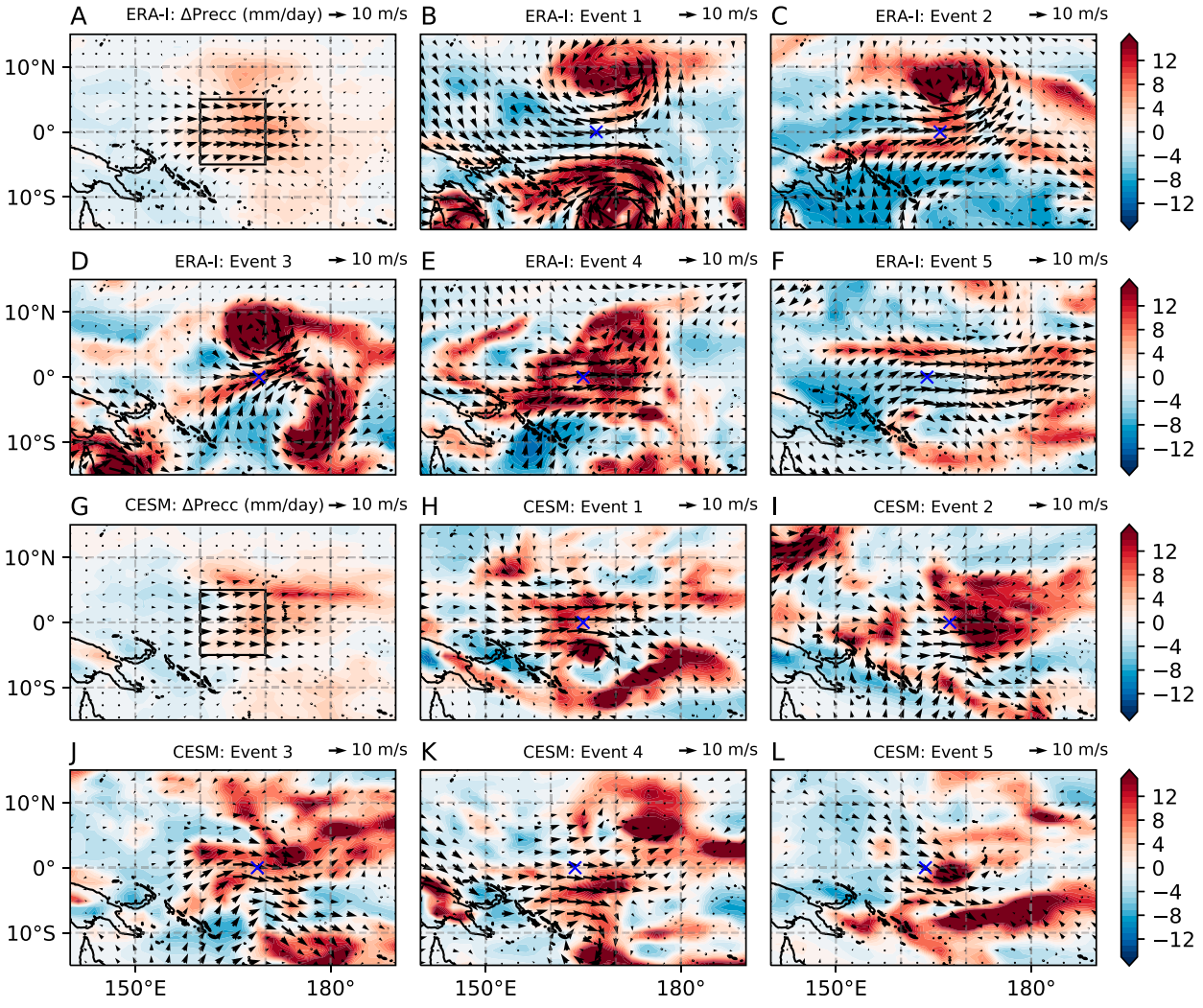

FIG. 5. Anomaly surface wind field (from climatology; arrows) and anomaly convective precipitation (from climatology; shading) for WWBs between 160° and 170°E in ERA-I, for (a) the composite and (b)–(f) the five strongest events in reanalysis. (g) As in (a), but for CESM; (h)–(l) as in (b)–(f), but for individual WWBs in CESM. Black boxes in (a) and (g) show regions where WWBs are composited, and the longitudinal position of the WWB center is marked by a blue cross.

mechanism in reanalysis, and it is not possible to verify that without being able to stop convection on and off the equator as we did in CESM.

Finally, to better understand the time evolution of the response to turning off convective heating on and off the equator, and the overall amplitude of the WWBs under the above described experiments, we plot Hovmöller diagrams of the zonal wind anomalies of composited and individual WWBs. We construct the plots for composited (Fig. 6, row 1) and individual (Fig. 6, rows 2–6) events, for the control (left column) and experiments where convective heating is disabled two days prior on the equator (center column) and off the equator (right column). Consistent with previous diagnostics, the center column shows that the overall development, amplitude, and propagation of a WWB is not strongly changed when convection is disabled on the equator (center column). On the other hand, when convection is disabled off-equator, the WWB is strongly suppressed in the longitude interval where the original event occurred (right column). We note that especially for those events exhibiting eastward propagation, a secondary event sometimes develops east of the date line, outside the eastern boundary of the boxes where convection is turned off (e.g., rows 2 and 5). We remark that from the composites, it is difficult to distinguish whether WWBs propagate east or west, as there appears to be a V-shaped pattern in the composite (see lighter shades of red, left column, row 1). Some events propagate strongly to the east (e.g., row 5) while others show a westward propagation (e.g., row 2). Nearly all WWBs have a weak westerly signal that propagates eastward (lighter shades of red, left column, row 1) outside of the domain of the WWB itself (shown by the solid black contour). This weak eastward propagating signal may be related to an atmospheric Kelvin

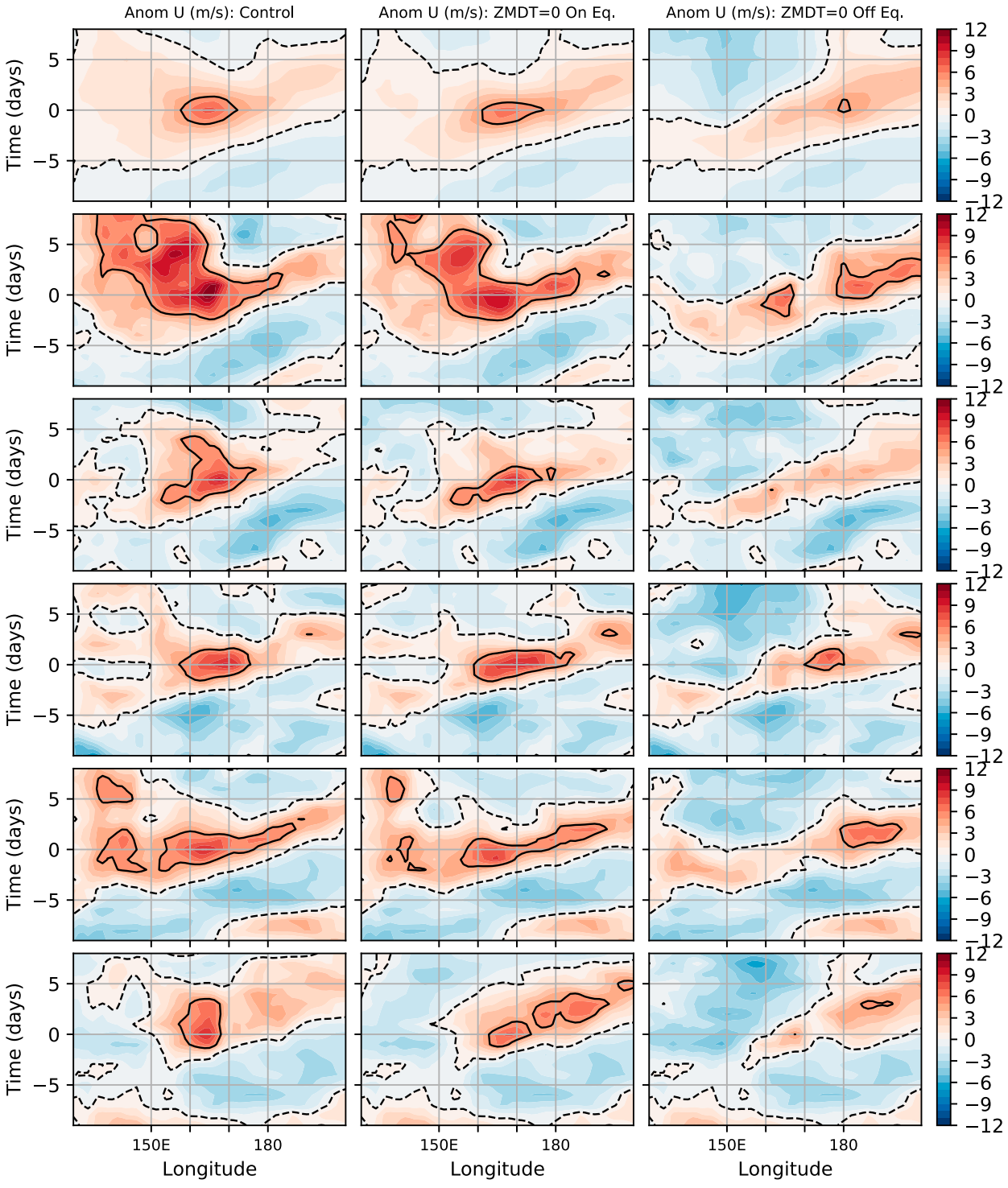

FIG. 6. Hovmöller diagrams of zonal wind anomalies between ±5° latitude (shading) for WWBs occurring between 160° and 170°E. Results are plotted for the (left) control experiment, and experiments where convective heating is turned off (center) near the equator or (right) off the equator two days before the peak of the event (day 0). The first row is a composite of the 25 events, and rows 2–6 show the five strongest individual events. The solid black contour corresponds to a 5 m s^{-1} anomaly zonal wind, while the dashed black contour denotes a 0 m s^{-1} anomaly zonal wind.

wave, as tropical cyclone tracks are generally westward at low latitudes. The diverse propagation characteristics of WWBs are a feature that should be evaluated more carefully in future studies.

In addition to the 25 WWBs occurring in the western-central Pacific (160°–170°E) in our 60-yr model run, we reproduced all analyses for the 17 WWBs occurring from 160° to 170°W, to verify our results are insensitive to the longitude at which WWBs occur (not shown). Indeed, we find the same qualitative results for all experiments. Minor differences are observed in the characteristics of WWBs occurring farther east. For instance, those WWBs occurring farther east are more likely to be caused by Northern Hemisphere cyclones, and their zonal wind anomalies generally do not show westward propagation. None of the differences change our conclusion, namely that off-equator moist convection drives tropical cyclones, which can in turn lead to WWBs on the equator.

4. Conclusions

The objective of this paper was to better understand the role that convection plays in the dynamics of *individual* WWBs. We studied the importance of convective heating and surface fluxes through an initial-value framework in which they are turned off selectively near individual developing WWBs. We found that off-equator convection is of greatest importance to the growth of individual WWBs, as disabling convective heating or evaporation just north and south of the central equatorial location of a developing WWB reduces surface wind vorticity and decreases the vortex's westerly anomaly near the equatorial region. This is consistent with Lian et al. (2018a).

These results complement those of Fu and Tziperman (2019), who used global mechanism denial experiments in which WISHE is turned off globally. They found that turning off WISHE globally reduced the number of WWBs dramatically in an *aquaplanet* model, and the results hinted, although did not prove, that WISHE may be amplifying individual events as well. We have shown here that WISHE, in fact, does not amplify individual events. Furthermore, as part of the current work, we performed experiments in which we set latent heat fluxes to climatology globally in a GCM with *realistic* boundary conditions, including the presence of continents and topography (not shown). Under these conditions, we find that the WWB strength and frequency are not significantly reduced. Our conclusion is that the global effect of WISHE on the statistics of WWBs is sensitive to model configuration, and this requires some additional work to decipher. It appears that off-equator convection, such as associated with tropical cyclones, is most important for explaining WWBs. More generally, the factors related to tropical cyclones may therefore be most important for creating and amplifying WWBs.

The double-cyclone structure associated with some WWBs has often been described as resembling the stationary Rossby wave pattern of the Gill response to an *equatorial* heat source (Fu and Tziperman 2019; Hartten 1996; Seiki and Takayabu 2007; Harrison and Giese 1991; Levine et al. 2017; Kubota et al. 2006; Lander 1990). For example, Lander (1990) described the importance of convection along the equator for initiating twin cyclones. Our results indicate that the double cyclones associated with WWBs are not a Gill response to on-equator (convective) heating, since we find that suppressing convection on the equator either through disabling evaporation or convective heating generally fails to disable a developing event. Instead, cyclonic vortices, whether on both sides of the equator or only one, associated with deep convection off the equator, appear to be the main processes driving WWBs.

We remark that our experiments do not rule out the possibility of surface flux feedbacks such as WISHE contributing to other forms of tropical variability, (e.g., MJO, atmospheric waves), that could impact WWBs indirectly. We do not address such indirect links in this paper, but note that this could be an interesting topic for future studies. Furthermore, although the coarse resolution of our model fails to properly resolve the full dynamics of tropical cyclones, many GCMs generate TC-like vortices with properties qualitatively similar to tropical cyclones (Camargo and Wing 2016). Combined with the fact that GCMs are able to model WWB statistics reasonably well (Lian et al. 2018b) and are able to generate such cyclonic vortices, our results are consistent with the view that cyclones or cyclone-like features may be of importance to the majority of WWBs. Furthermore, we demonstrate that the convection observed in those cyclonic vortices is best understood as an active part of the WWB mechanism rather than as a forced response to near-equator convection.

Acknowledgments. This research was supported by the NSF Climate Dynamics program Grants AGS-1924538 and AGS-1826635, and by the Harvard-UTEC fund. Eli Tziperman thanks the Weizmann Institute for its hospitality during parts of this work. We thank three anonymous reviewers for their helpful comments. We would like to acknowledge high-performance computing support from Cheyenne (doi:10.5065/D6RX99HX) provided by NCAR's Computational and Information Systems Laboratory, sponsored by the National Science Foundation.

Data availability statement. Source code modifications and postprocessing scripts are available at https://osf.io/cznqy/. Dataset access is listed as follows. CESM Large Ensemble: http://www.cesm.ucar.edu/projects/community-projects/LENS/data-sets.html. ERA-Interim: https://www.ecmwf.int/en/forecasts/datasets/reanalysis-datasets/era-interim.

REFERENCES

Camargo, S. J., and A. A. Wing, 2016: Tropical cyclones in climate models. *Wiley Interdiscip. Rev.: Climate Change*, **7**, 211–237, https://doi.org/10.1002/wcc.373.

Chen, S., R. Houze, and B. Mapes, 1996: Multiscale variability of deep convection in relation to large-scale circulation in TOGA COARE. *J. Atmos. Sci.*, **53**, 1380–1409, https://doi.org/10.1175/1520-0469(1996)053<1380:MVODCI>2.0.CO;2.

Chiodi, A. M., D. E. Harrison, and G. A. Vecchi, 2014: Subseasonal atmospheric variability and El Niño waveguide warming: Observed effects of the Madden–Julian oscillation and westerly wind events. *J. Climate*, **27**, 3619–3642, https://doi.org/10.1175/JCLI-D-13-00547.1.

Chu, P.-S., 1988: Extratropical forcing and the burst of equatorial westerlies in the western Pacific: A synoptic study. *J. Meteor. Soc. Japan*, **66**, 549–564, https://doi.org/10.2151/jmsj1965.66.4_549.

Dee, D. P., and Coauthors, 2011: The ERA-Interim reanalysis: Configuration and performance of the data assimilation system. *Quart. J. Roy. Meteor. Soc.*, **137**, 553–597, https://doi.org/10.1002/qj.828.

Eisenman, I., L. S. Yu, and E. Tziperman, 2005: Westerly wind bursts: ENSO's tail rather than the dog? *J. Climate*, **18**, 5224–5238, https://doi.org/10.1175/JCLI3588.1.

Fasullo, J., and P. J. Webster, 2000: Atmospheric and surface variations during westerly wind bursts in the tropical western Pacific. *Quart. J. Roy. Meteor. Soc.*, **126**, 899–924, https://doi.org/10.1002/qj.49712656407.

Feng, J., and T. Lian, 2018: Assessing the relationship between MJO and equatorial Pacific WWBS in observations and CMIP5 models. *J. Climate*, **31**, 6393–6410, https://doi.org/10.1175/JCLI-D-17-0526.1.

Fu, M., and E. Tziperman, 2019: Essential ingredients to the dynamics of westerly wind bursts. *J. Climate*, **32**, 5549–5565, https://doi.org/10.1175/JCLI-D-18-0584.1.

Gebbie, G., and E. Tziperman, 2009a: Incorporating a semi-stochastic model of ocean-modulated westerly wind bursts into an ENSO prediction model. *Theor. Appl. Climatol.*, **97**, 65–73, https://doi.org/10.1007/s00704-008-0069-6.

——, and ——, 2009b: Predictability of SST-modulated westerly wind bursts. *J. Climate*, **22**, 3894–3909, https://doi.org/10.1175/2009JCLI2516.1.

——, I. Eisenman, A. T. Wittenberg, and E. Tziperman, 2007: Modulation of westerly wind bursts by sea surface temperature: A semi-stochastic feedback for ENSO. *J. Atmos. Sci.*, **64**, 3281–3295, https://doi.org/10.1175/JAS4029.1.

Giese, B., and D. Harrison, 1991: Eastern equatorial Pacific response to three composite westerly wind types. *J. Geophys. Res.*, **96** (Suppl.), 3239–3248, https://doi.org/10.1029/90JC01861.

Gill, A. E., 1980: Some simple solutions for heat-induced tropical circulation. *Quart. J. Roy. Meteor. Soc.*, **106**, 447–462, https://doi.org/10.1002/qj.49710644905.

Harrison, D. E., and B. S. Giese, 1991: Episodes of surface westerly winds as observed from islands in the western tropical Pacific. *J. Geophys. Res. Oceans*, **96**, 3221–3237, https://doi.org/10.1029/90JC01775.

——, and G. A. Vecchi, 1997: Westerly wind events in the tropical Pacific, 1986–95. *J. Climate*, **10**, 3131–3156, https://doi.org/10.1175/1520-0442(1997)010<3131:WWEITT>2.0.CO;2.

Hartten, L. M., 1996: Synoptic settings of westerly wind bursts. *J. Geophys. Res.*, **101**, 16 997–17 019, https://doi.org/10.1029/96JD00030.

Jin, F.-F., L. Lin, A. Timmermann, and J. Zhao, 2007: Ensemble-mean dynamics of the ENSO recharge oscillator under state-dependent stochastic forcing. *Geophys. Res. Lett.*, **34**, L03807, https://doi.org/10.1029/2006GL027372.

Kay, J. E., and Coauthors, 2015: The Community Earth System Model (CESM) large ensemble project: A community resource for studying climate change in the presence of internal climate variability. *Bull. Amer. Meteor. Soc.*, **96**, 1333–1349, https://doi.org/10.1175/BAMS-D-13-00255.1.

Keen, R. A., 1982: The role of cross-equatorial tropical cyclone pairs in the southern oscillation. *Mon. Wea. Rev.*, **110**, 1405–1416, https://doi.org/10.1175/1520-0493(1982)110<1405:TROCET>2.0.CO;2.

Kessler, W. S., M. J. McPhaden, and K. M. Weickmann, 1995: Forcing of intraseasonal Kelvin waves in the equatorial Pacific. *J. Geophys. Res.*, **100**, 10 613–10 631, https://doi.org/10.1029/95JC00382.

Kiladis, G. N., and M. Wheeler, 1995: Horizontal and vertical structure of observed tropospheric equatorial Rossby waves. *J. Geophys. Res.*, **100**, 22 981–22 997, https://doi.org/10.1029/95JD02415.

——, G. A. Meehl, and K. M. Weickmann, 1994: Large-scale circulation associated with westerly wind bursts and deep convection over the western equatorial Pacific. *J. Geophys. Res.*, **99**, 18 527–18 544, https://doi.org/10.1029/94JD01486.

Kleeman, R., and A. M. Moore, 1997: A theory for the limitation of ENSO predictability due to stochastic atmospheric transients. *J. Atmos. Sci.*, **54**, 753–767, https://doi.org/10.1175/1520-0469(1997)054<0753:ATFTLO>2.0.CO;2.

Kubota, H., R. Shirooka, T. Ushiyama, J. Chen, T. Chuda, K. Takeuchi, K. Yoneyama, and M. Katsumata, 2006: Observations of the structures of deep convections and their environment during the active phase of an Madden-Julian oscillation event over the equatorial western Pacific. *J. Meteor. Soc. Japan*, **84**, 115–128, https://doi.org/10.2151/jmsj.84.115.

Lander, M. A., 1990: Evolution of the cloud pattern during the formation of tropical cyclone twins symmetrical with respect to the equator. *Mon. Wea. Rev.*, **118**, 1194–1202, https://doi.org/10.1175/1520-0493(1990)118<1194:EOTCPD>2.0.CO;2.

Latif, M., J. Biercamp, and H. von Storch, 1988: The response of a coupled ocean–atmosphere general circulation model to wind bursts. *J. Atmos. Sci.*, **45**, 964–979, https://doi.org/10.1175/1520-0469(1988)045<0964:TROACO>2.0.CO;2.

Lengaigne, M., E. Guilyardi, J. P. Boulanger, C. Menkes, P. Delecluse, P. Inness, J. Cole, and J. Slingo, 2004: Triggering of El Niño by westerly wind events in a coupled general circulation model. *Climate Dyn.*, **23**, 601–620, https://doi.org/10.1007/s00382-004-0457-2.

Levine, A. F., F. F. Jin, and M. F. Stuecker, 2017: A simple approach to quantifying the noise–ENSO interaction. Part II: The role of coupling between the warm pool and equatorial zonal wind anomalies. *Climate Dyn.*, **48**, 19–37, https://doi.org/10.1007/s00382-016-3268-3.

Lian, T., D. Chen, Y. Tang, X. Liu, J. Feng, and L. Zhou, 2018a: Linkage between westerly wind bursts and tropical cyclones. *Geophys. Res. Lett.*, **45**, 11 431–11 438, https://doi.org/10.1029/2018GL079745.

——, Y. Tang, L. Zhou, S. U. Islam, C. Zhang, X. Li, and Z. Ling, 2018b: Westerly wind bursts simulated in CAM4 and CCSM4. *Climate Dyn.*, **50**, 1353–1371, https://doi.org/10.1007/s00382-017-3689-7.

Luther, D. S., D. E. Harrison, and R. A. Knox, 1983: Zonal winds in the central equatorial Pacific and El Niño. *Science*, **222**, 327–330, https://doi.org/10.1126/science.222.4621.327.

McPhaden, M. J., F. Bahr, Y. Du Penhoat, E. Firing, S. Hayes, P. Niiler, P. Richardson, and J. Toole, 1992: The response of the western equatorial Pacific Ocean to westerly wind bursts during November 1989 to January 1990. *J. Geophys. Res. Oceans*, **97**, 14 289–14 303, https://doi.org/10.1029/92JC01197.

Meehl, G. A., G. N. Kiladis, K. M. Weickmann, M. Wheeler, D. S. Gutzler, and G. P. Compo, 1996: Modulation of equatorial subseasonal convective episodes by tropical–extratropical interaction in the Indian and Pacific Ocean regions. *J. Geophys. Res.*, **101**, 15 033–15 049, https://doi.org/10.1029/96JD01014.

Moore, A. M., and R. Kleeman, 1997a: The singular vectors of a coupled ocean–atmosphere model of ENSO. I: Thermodynamics, energetics and error growth. *Quart. J. Roy. Meteor. Soc.*, **123**, 953–981, https://doi.org/10.1002/qj.49712354009.

——, and ——, 1997b: The singular vectors of a coupled ocean-atmosphere model of ENSO. II: Sensitivity studies and dynamical interpretation. *Quart. J. Roy. Meteor. Soc.*, **123**, 983–1006, https://doi.org/10.1002/qj.49712354010.

——, and ——, 1999: The nonnormal nature of El Niño and intraseasonal variability. *J. Climate*, **12**, 2965–2982, https://doi.org/10.1175/1520-0442(1999)012<2965:TNNOEN>2.0.CO;2.

——, and ——, 2001: The differences between the optimal perturbations of coupled models of ENSO. *J. Climate*, **14**, 138–163, https://doi.org/10.1175/1520-0442(2001)014<0138:TDBTOP>2.0.CO;2.

Nitta, T., 1989: Development of a twin cyclone and westerly bursts during the initial phase of the 1986–87 El Niño. *J. Meteor. Soc. Japan*, **67**, 677–681, https://doi.org/10.2151/jmsj1965.67.4_677.

Penland, C., and P. D. Sardeshmukh, 1995: The optimal growth of tropical sea surface temperature anomalies. *J. Climate*, **8**, 1999–2024, https://doi.org/10.1175/1520-0442(1995)008<1999:TOGOTS>2.0.CO;2.

Perez, C. L., A. M. Moore, J. Zavala-Garay, and R. Kleeman, 2005: A comparison of the influence of additive and multiplicative stochastic forcing on a coupled model of ENSO. *J. Climate*, **18**, 5066–5085, https://doi.org/10.1175/JCLI3596.1.

Perigaud, C. M., and C. Cassou, 2000: Importance of oceanic decadal trends and westerly wind bursts for forecasting El Niño. *Geophys. Res. Lett.*, **27**, 389–392, https://doi.org/10.1029/1999GL010781.

Puy, M., J. Vialard, M. Lengaigne, and E. Guilyardi, 2016: Modulation of equatorial Pacific westerly/easterly wind events by the Madden–Julian oscillation and convectively-coupled Rossby waves. *Climate Dyn.*, **46**, 2155–2178, https://doi.org/10.1007/s00382-015-2695-x.

Seiki, A., and Y. N. Takayabu, 2007: Westerly wind bursts and their relationship with intraseasonal variations and ENSO. Part I: Statistics. *Mon. Wea. Rev.*, **135**, 3325–3345, https://doi.org/10.1175/MWR3477.1.

Sura, P., and P. D. Sardeshmukh, 2008: A global view of non-Gaussian SST variability. *J. Phys. Oceanogr.*, **38**, 639–647, https://doi.org/10.1175/2007JPO3761.1.

Tziperman, E., and L. Yu, 2007: Quantifying the dependence of westerly wind bursts on the large-scale equatorial Pacific SST. *J. Climate*, **20**, 2760–2768, https://doi.org/10.1175/JCLI4138a.1.

Vecchi, G., and D. Harrison, 2000: Tropical Pacific sea surface temperature anomalies, El Niño and equatorial westerly wind events. *J. Climate*, **13**, 1814–1830, https://doi.org/10.1175/1520-0442(2000)013<1814:TPSSTA>2.0.CO;2.

Yu, L., R. A. Weller, and T. W. Liu, 2003: Case analysis of a role of ENSO in regulating the generation of westerly wind bursts in the western equatorial Pacific. *J. Geophys. Res.*, **108**, 3128, https://doi.org/10.1029/2002JC001498.

Zhang, C. D., 1996: Atmospheric intraseasonal variability at the surface in the tropical western Pacific Ocean. *J. Atmos. Sci.*, **53**, 739–758, https://doi.org/10.1175/1520-0469(1996)053<0739:AIVATS>2.0.CO;2.

Zhang, G. J., and N. A. McFarlane, 1995: Sensitivity of climate simulations to the parameterization of cumulus convection in the Canadian Climate Centre general circulation model. *Atmos.–Ocean*, **33**, 407–446, https://doi.org/10.1080/07055900.1995.9649539.